Journal of Food Measurement and Characterization
https://doi.org/10.1007/s11694-026-04579-1

ORIGINAL PAPER

Convolutional neural networks for predicting moisture ratio from images of beetroot cubes under different drying pretreatments

Suian José Granella[1] · Marina Barros Zacharias[1] · Tiago Bueno de Moraes[1]

Received: 3 December 2025 / Accepted: 1 June 2026
© The Author(s) 2026, modified publication 2026

Abstract
This study proposes a proof-of-concept approach for predicting the mean moisture ratio of beetroot cubes directly from RGB images acquired during convective drying under different pretreatments and air temperatures. Beetroot (*Beta vulgaris* L.) cubes were subjected to four pretreatments: control (BC), ethanol immersion (BE), ultrasound in water (BCU), and combined ethanol + ultrasound (BEU), and dried at 60, 70, and 80 °C. During drying, RGB images of individual cubes were recorded synchronously with gravimetric measurements. A custom convolutional neural network (cnn1v) was developed to perform regression from RGB images to moisture ratio. On the independent test set, the model achieved a global performance of $R^2 \approx 0.29$, MAE of 0.29, and RMSE of 0.32, indicating moderate overall predictive capability. However, condition-wise analysis revealed substantially higher performance under specific regimes, with $R^2 > 0.90$ and MAE < 0.10 for BE at 70–80 °C and BCU at 60 °C, while the combined BEU pretreatment exhibited the lowest accuracy across all temperatures. These results demonstrate that the cnn1v model is able to capture meaningful drying trajectories from simple RGB images under controlled conditions, but its performance is strongly dependent on pretreatment and drying regime. The findings highlight both the potential and limitations of low-cost vision-based monitoring for drying processes.

Keywords Convolutional neural networks · Deep learning · Moisture ratio · Beetroot cubes · Convective drying · Non-destructive monitoring

Introduction

Drying is one of the most widely used preservation methods in the food and agricultural sectors, as it reduces water activity, extends shelf-life and decreases transportation and storage costs. However, the drying process can strongly affect the physical, chemical and sensory quality of plant-based products, especially those rich in pigments and bioactive compounds [1, 2], such as beetroot (Beta vulgaris L.). Ethanol and ultrasound pretreatments have been proposed as intensification strategies to shorten drying time and mitigate quality losses by altering cell structure, enhancing mass transfer and reducing energy consumption [3, 4].

The design and control of drying processes traditionally rely on empirical models (e.g. Page-type equations) or on Fickian diffusion-based formulations, which describe moisture migration inside the product. While these approaches provide useful engineering insight, they require precise measurements of moisture content over time and may not fully capture complex structural changes during drying [5, 6]. In parallel, the increasing availability of digital imaging and computational power has opened new possibilities for non-destructive monitoring of drying, by linking visual attributes such as color and surface texture to internal moisture content.

Recent studies have demonstrated the potential of advanced optical sensing to achieve this goal in a wide range of products and drying configurations. Infrared thermography combined with irreversible thermodynamic modeling has been used to monitor convective drying of goldenberry (*Physalis peruviana*), enabling real-time tracking of surface

✉ Suian José Granella
granella@usp.br

Marina Barros Zacharias
marianazacharias@usp.br

Tiago Bueno de Moraes
tiago.moraes@usp.br

[1] Department of Biosystems Engineering (LEB), Luiz de Queiroz College of Agriculture (ESALQ), University of São Paulo (USP), Piracicaba, SP, Brazil

Published online: 16 June 2026

temperature and emissivity and linking these measurements to internal water flux and changes in water potential [7]. Hyperspectral imaging (HSI) and 3D point cloud data have been successfully integrated with machine learning to predict moisture content and bioactive compound retention during drying of purple carrot and golden kiwifruit, with Gaussian Process Regression and Gradient Boosting models reaching R^2_p values above 0.95 for moisture content and high accuracy for carotenoids and vitamin C [8]. Similar multisensor approaches combining FTIR spectroscopy, multispectral imaging and chemometrics have been applied to puffed dried apples, allowing non-destructive prediction of color and textural attributes and highlighting structural changes induced by drying [9]. In microwave vacuum dehydration of banana slices, near-infrared HSI and terahertz time-domain spectroscopy (THz-TDS) have shown strong capability for real-time moisture monitoring, yielding R^2 values above 0.90 for moisture loss prediction under different non-thermal pretreatments [10]. Laser light backscattering imaging, coupled with hand-crafted color and shape descriptors and deep features extracted by pre-trained CNNs, has also provided accurate prediction of moisture content in quince slices during hot-air drying [11]. Beyond drying, HSI combined with machine learning has been used to estimate moisture content and texture in sweet potato with high precision ($R^2 \approx 0.97$), reinforcing the relevance of image-based, data-driven approaches for assessing quality and water status in agro-food matrices [12]. Collectively, these works show that optical and spectroscopic imaging, when coupled with suitable learning algorithms, can deliver accurate, non-destructive estimates of moisture and quality attributes, motivating the exploration of simpler RGB-based CNN models for monitoring drying processes.

Convolutional neural networks (CNNs) have become the state-of-the-art approach for image analysis in various domains, including food quality assessment, defect detection and classification of horticultural products. Unlike hand-crafted feature extraction, CNNs automatically learn hierarchical representations directly from pixels, which can capture subtle visual cues associated with moisture loss, shrinkage and surface roughness.

In this context, the objective of the present work was to evaluate the capability of a CNN-based model to predict the mean moisture ratio of beetroot cubes from RGB images acquired during convective drying under different pretreatment conditions. Beetroot cubes were subjected to four treatments (control, ethanol, ultrasound, and ultrasound combined with ethanol) and dried at distinct drying air temperatures (60–80 °C). A custom CNN architecture (cnn1v) was trained to perform regression from images to the mean moisture ratio, and its performance was assessed using standard error metrics and graphical analysis of observed versus predicted drying curves. The study is proposed as a proof-of-concept for image-based monitoring of drying processes in pretreated plant materials.

Material and methods

Raw material and sample preparation

Fresh beetroot (*Beta vulgaris* L.) roots were obtained from a local market and selected based on visual uniformity in size and colour, and the absence of mechanical damage or disease symptoms. The beetroots were manually peeled and cut into cubes using a cutting jig to ensure consistent dimensions (approximately $10 \times 10 \times 10$ mm). After cutting, a representative subsample of cubes was used to determine the initial moisture content by oven drying at $105\,^{\circ}\mathrm{C}$ until constant mass, resulting in an initial moisture content of 88.64% (wet basis). The remaining cubes were kept covered to minimize dehydration prior to the pretreatments and drying experiments. All sample handling was conducted at room temperature ($\approx 20\,^{\circ}\mathrm{C}$).

Pretreatment prior to drying

Four pretreatment conditions were evaluated prior to convective drying: control without pretreatment (BC), ethanol immersion (BE), ultrasound in aqueous medium (BCU), and combined ultrasound plus ethanol (BEU).

For the control treatment (BC), beetroot cubes were directly loaded into the dryer without any prior immersion or ultrasound exposure. In the ethanol pretreatment (BE), cubes were immersed in an ethanol solution at a concentration of 50% (v/v) for $t_E = 15$ min under gentle agitation and then drained on absorbent paper to remove excess surface liquid.

For the ultrasound pretreatment (BCU), cubes were immersed in distilled water and subjected to ultrasonic waves in a bath operating at a nominal frequency of 20 kHz and power of 50 W for a predetermined time t_U. In the combined pretreatment (BEU), ethanol immersion and ultrasound were applied simultaneously, using the same operating conditions described above. After pretreatment, all samples were briefly drained and immediately transferred to the convective dryer.

Figure 1 presents a schematic representation of the experimental procedure used for the application of the drying pretreatments.

Convective drying

Convective drying experiments were carried out in a laboratory-scale tray dryer (model SL102, Solab, Brazil) equipped

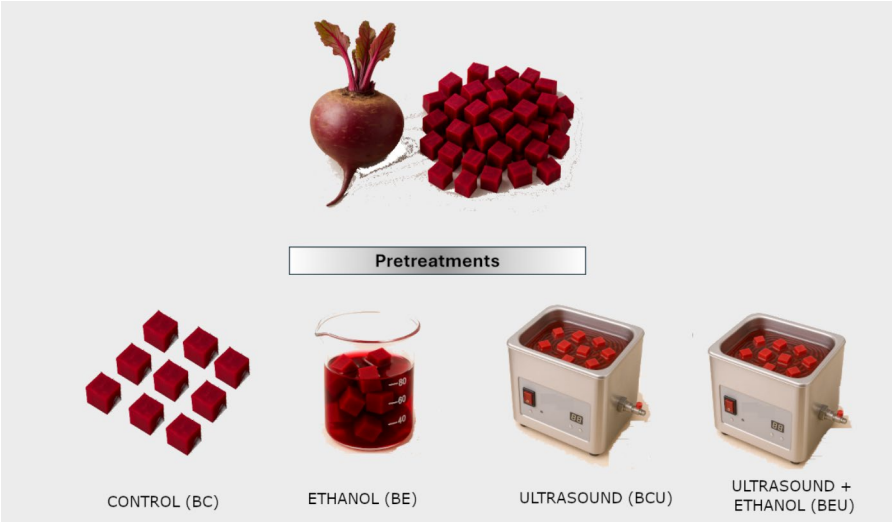


Fig. 1 Schematic representation of the experimental procedure for the application of the drying pretreatments: control (BC), ethanol immersion (BE), ultrasound in water (BCU), and combined ultrasound plus ethanol (BEU)

with temperature and air-velocity control. The beetroot cubes were arranged in a single layer on perforated trays, ensuring that the cubes did not touch each other so as to avoid shadowing and uneven airflow.

Drying was performed at air temperatures of 60, 70, and 80 °C, with an air velocity of approximately 1.2 m s^{-1} and ambient relative humidity of $49.6 \pm 3.6\%$. For each combination of pretreatment and temperature, at least three independent drying runs were conducted.

During each run, the trays were periodically removed from the dryer at predetermined time intervals, and the sample mass was recorded using an analytical balance with a resolution of 0.01 g. The trays were returned to the dryer immediately after weighing to minimize temperature fluctuations. Drying was continued until the mass change between two consecutive measurements was negligible, indicating that the samples had approached the equilibrium moisture content.

Moisture ratio determination

The moisture content of the beetroot cubes at each drying time was calculated from the mass measurements, assuming that dry matter remained constant throughout the process. The moisture content on a dry basis, X_t (kg water/kg dry matter), at time t was obtained from the initial and time-dependent sample masses and the dry mass determined at the end of drying.

The dimensionless moisture ratio (moisture ratio, MR) was computed according to:

$$\mathrm{MR} = \frac{X_t - X_{\mathrm{eq}}}{X_0 - X_{\mathrm{eq}}}, \tag{1}$$

where X_0 is the initial moisture content (dry basis) and X_{eq} is the equilibrium moisture content. When X_{eq} was small compared with X_0 and X_t, it was approximated as zero, as commonly adopted in drying studies.

Image acquisition and preprocessing

RGB images of the beetroot cubes were acquired synchronously with the gravimetric measurements during drying. A Samsung Galaxy A54 smartphone (rear camera, Samsung Electronics Co., South Korea) was mounted on a fixed support above the drying tray at a distance of approximately 25 cm, with the optical axis perpendicular to the tray surface. A uniform matte white background and controlled illumination (LED light source with a color temperature of 5500 K) were used to minimize shadows and reflections and to ensure consistent imaging conditions across all experiments.

At each sampling time, a photograph of the tray containing the cubes was captured and stored in JPEG format with an original resolution of 3060×4080 pixels. Afterwards, individual cube regions were manually or semi-automatically cropped from the original images based on their known positions on the tray, generating a dataset of single-cube images. All images were resized to 224×224 pixels and normalised prior to being fed to the CNN. Pixel intensities were scaled to the [0, 1] range using a rescaling layer in the deep-learning pipeline.

The final dataset was organized by associating each processed image with the corresponding mean moisture ratio (rm_mean), pretreatment (BC, BE, BCU, BEU), drying temperature, and time. The complete dataset was then randomly split into training (70%), validation (15%), and test (15%) subsets, ensuring that images from the same experimental condition were appropriately represented across the subsets to support model training and evaluation.

In total, between 11 and 15 images were acquired for each replicate of a given drying condition. Image acquisition started at 5 min intervals and the interval was gradually increased as drying progressed, until the samples reached equilibrium moisture content (constant mass).

Visualization of convolutional feature maps

To qualitatively inspect the features learned by the CNN, activation maps from the first convolutional layer were extracted for a representative RGB image of beetroot cubes under convective drying conditions. The trained cnn1v model was evaluated in inference mode, and the output tensor of the first convolutional layer was visualized.

A subset of six feature channels (filters 0–5) was selected for interpretation. Each activation map represents the spatial response of the corresponding filter to local intensity variations, edges, and texture discontinuities in the input image. The maps were visualized as two-dimensional heatmaps using a continuous color scale in `matplotlib`.

As shown in Fig. 2, different filters respond to distinct visual patterns. Some filters act as edge detectors, highlighting the boundaries of beetroot cubes and their shrinkage-induced deformation. Others emphasize internal texture variations and local intensity gradients associated with surface roughness and moisture-dependent color changes during drying. Filters with weak activation indicate redundancy or low sensitivity to the selected input features.

Convolutional neural network architecture (cnn1v) and training procedure

A convolutional neural network (CNN), hereafter referred to as *cnn1v*, was developed to perform regression from RGB images of beetroot cubes to the corresponding mean moisture ratio ($\mathrm{rm_mean}$). For each image, $\mathrm{rm_mean}$ was calculated as the arithmetic mean of three experimental repetitions (rm1, rm2 and rm2.1), as described in "Moisture ratio determination" section, and used as the target variable in the learning task. The input to the network consisted of resized single-cube images with a spatial resolution of 224×224 pixels and three colour channels (RGB). Pixel values were scaled to the [0, 1] range by means of a `Rescaling` layer placed at the network input.

The *cnn1v* architecture comprised three convolutional blocks followed by a fully connected head. Each convolutional block consisted of a two-dimensional convolutional layer with 3×3 kernels, rectified linear unit (ReLU) activation and *same* padding, followed by 2×2 max-pooling for spatial downsampling. The numbers of filters in the three convolutional layers were 32, 64 and 128, respectively. After the convolutional blocks, the resulting feature maps

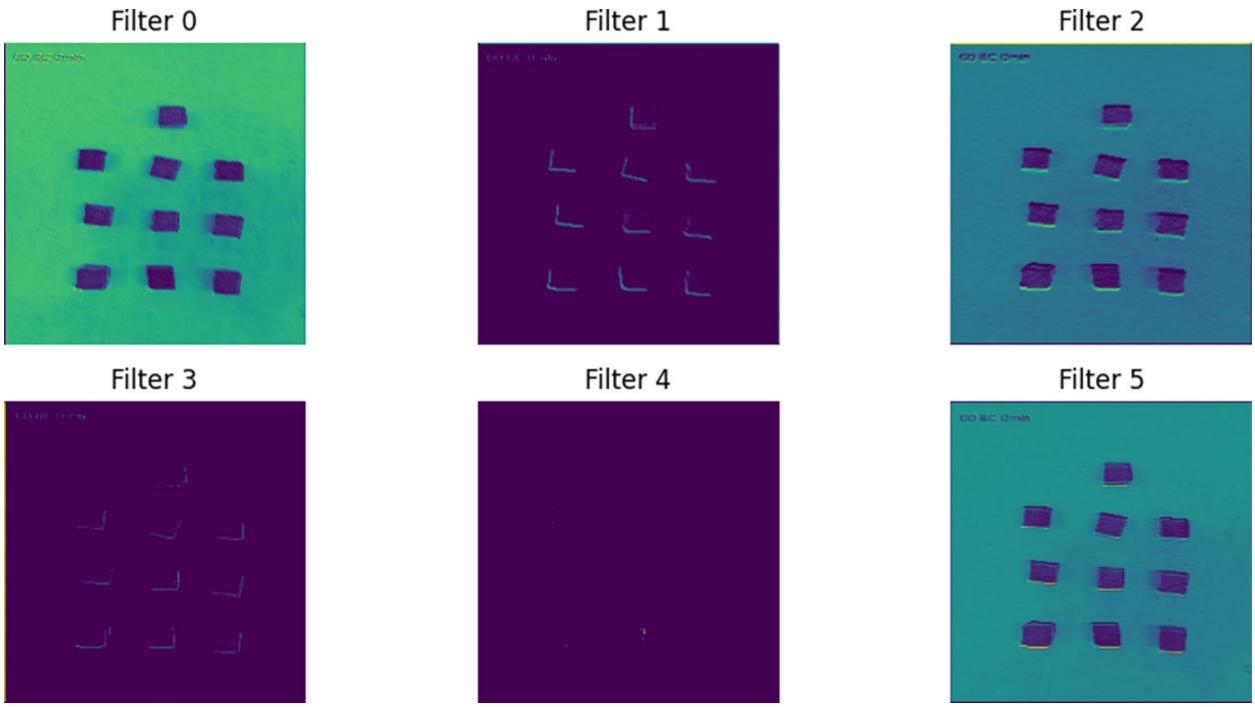


Fig. 2 Activation maps of the first convolutional layer (filters 0–5) for a representative beetroot cube image under convective drying. Each panel shows the spatial response of a convolutional filter to edges, texture variations, and intensity gradients associated with shrinkage and moisture loss. These features reflect early-stage hierarchical representations learned by the cnn1v model

were flattened and fed into a dense layer with 128 neurons and ReLU activation, followed by a dropout layer with a dropout rate of 0.5 to mitigate overfitting. The output layer consisted of a single neuron with linear activation, providing the predicted $\mathrm{rm_mean}$ value.

The model was implemented in Python using TensorFlow/Keras. The dataset of images and associated $\mathrm{rm_mean}$ values was partitioned at the *experimental run level*, meaning that all images belonging to the same drying run (specific combination of pretreatment and temperature) were assigned exclusively to either the training, validation, or test set. This strategy was adopted to avoid data leakage between subsets and to ensure an unbiased evaluation of model generalization.

The dataset was divided into training (70%), validation (15%), and test (15%) subsets using a fixed random seed to ensure reproducibility. The distribution of pretreatments and drying temperatures was approximately preserved across the subsets.

Given the limited number of samples per experimental condition, mild data augmentation was applied only to the training set to improve model robustness. The augmentation strategy included random horizontal flipping and small variations in brightness. No geometric transformations that could alter the physical interpretation of the drying process were applied. It is important to emphasize that data augmentation was used solely to improve robustness to minor illumination variability and does not replace the need for larger and more diverse experimental datasets.

Training was carried out with mini-batches of 32 images, using the Adam optimizer with default hyperparameters and mean squared error (MSE) as the loss function. In addition to the loss, mean absolute error (MAE), MSE and a custom coefficient of determination (R^2) were monitored as performance metrics. The network was trained for 34 epochs while monitoring the validation loss, and the training history (training and validation MSE and MAE versus epoch) was recorded for subsequent analysis of convergence behavior and potential overfitting.

Model evaluation and statistical analysis

The predictive performance of the `cnn1v` model was evaluated on the independent test subset using standard regression metrics: mean absolute error (MAE), mean squared error (MSE), root mean squared error (RMSE) and the coefficient of determination (R^2). Global metrics were computed for the entire test set, and additional analyzes were carried out by conditioning on pretreatment type (BC, BE, BCU and BEU) and drying temperature, in order to assess possible differences in performance across experimental conditions.

To assess the agreement between observed and predicted values, scatter plots of observed versus CNN-predicted were constructed, including the 1:1 reference line. For a more process-oriented analysis, drying curves were reconstructed for selected combinations of pretreatment and temperature, comparing experimental data with CNN-predicted curves. All data processing, model training and statistical analyzes were performed in Python, using TensorFlow/Keras for deep learning, `scikit-learn` for computation of regression metrics, and `matplotlib` for visualization.

Results and discussion

Figure 3 illustrates the visual evolution of beetroot cubes during convective drying as a function of pretreatment and air temperature. In all cases, drying led to progressive darkening, shrinkage and surface roughening of the cube surfaces, but the intensity and kinetics of these changes clearly depended on both the pretreatment and the drying temperature. At lower temperatures (60 °C), color changes were more gradual and the cubes generally preserved a more regular shape for longer times, whereas at 80 °C the samples tended to darken rapidly and develop pronounced surface wrinkling and collapse. Ethanol and ultrasound pretreatments (BE, BCU and BEU) produced more heterogeneous textures and visible microcracks than the control (BC), suggesting that these treatments modify the microstructure and facilitate moisture removal. These qualitative observations support the hypothesis that RGB images contain meaningful visual cues related to the internal moisture state, which motivates the use of convolutional neural networks to predict the mean moisture ratio directly from the drying images.

These trends are consistent with previous optical monitoring studies in which drying induces spatially heterogeneous color changes and shrinkage patterns associated with moisture removal and microstructural damage. For instance, hyperspectral and 3D point cloud imaging of purple carrot and golden kiwifruit revealed decreasing chroma, increasing browning index and marked surface area reduction over time, particularly at higher temperatures [8].

Although the present work does not quantify geometrical changes, qualitative inspection of Fig. 3 suggests that ultrasound- and ethanol-based pretreatments (BCU and BEU) promote faster apparent dehydration than the control (BC), especially at 70 and 80 °C, as indicated by earlier onset of intense darkening and pronounced shrinkage. Similar acceleration of drying has been reported for ultrasound-assisted osmotic dehydration of banana slices during microwave vacuum dehydration, in which osmotic and ultrasound-osmotic pretreatments significantly increased moisture content loss and reduced browning compared with untreated samples

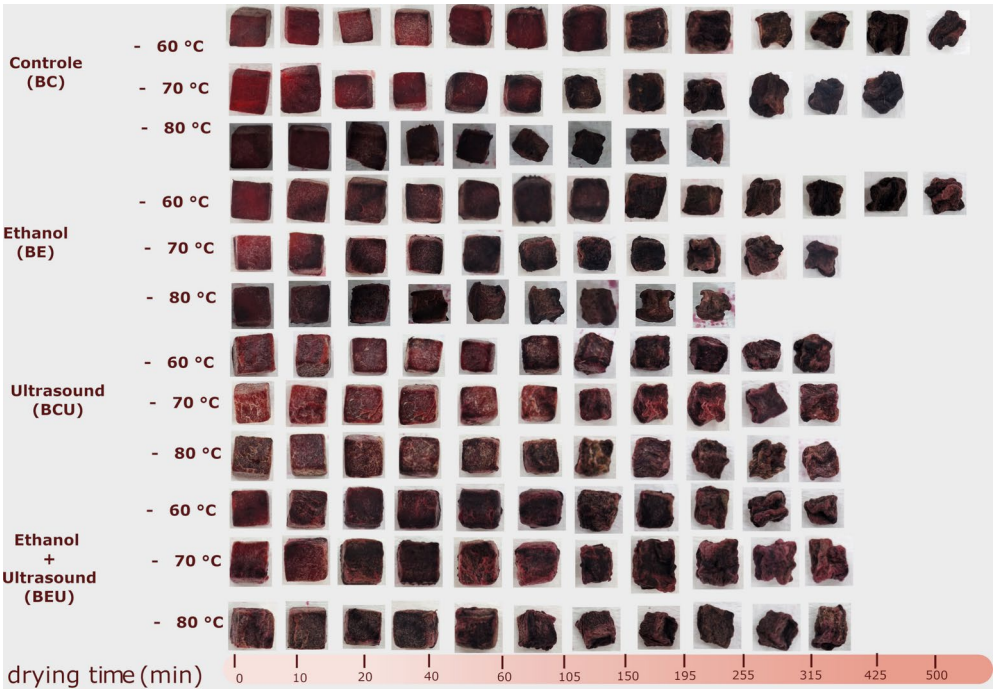


Fig. 3 Visual evolution of beetroot cubes during convective drying under different pretreatments and air temperatures. Rows correspond to the four pretreatments: control (BC), ethanol immersion (BE), ultrasound in water (BCU) and combined ethanol + ultrasound (BEU). For each pretreatment, drying was performed at 60, 70 and 80 °C. Columns represent representative drying times from 0 to 500 min, as indicated by the time axis at the bottom. Progressive darkening, shrinkage and surface roughening can be observed, with the intensity and kinetics of the visual changes depending on both pretreatment and drying temperature

[10]. These visual patterns reinforce the expectation that surface color and texture carry information about internal moisture status and motivate the use of image-based models to infer the moisture ratio non-destructively.

Drying curves: observed versus CNN-predicted moisture ratio

Figure 4 compares the experimental drying curves with the values predicted by the cnn1v model for all combinations of pretreatment (rows) and air temperature (columns). Each panel (A–L) shows the evolution of the moisture ratio as a function of drying time, together with the error metrics (MAE, RMSE, MSE and R^2) for the corresponding condition. Overall, the CNN was able to reproduce the characteristic decrease in moisture ratio over time, but the quality of the fit varied markedly among pretreatments and temperatures.

For the control treatment (BC; panels A–C), the model reasonably captured the overall trend of the drying curves, with R^2 values between approximately 0.59 and 0.78 and RMSE in the range 0.20–0.23. At 60 °C (panel A), the predictions follow the experimental curve for most of the process, although deviations appear at intermediate times. At 70 °C (panel B), the model underestimates the curvature of the experimental data, resulting in the lowest R^2 within the BC group. At 80 °C (panel C), the agreement improves again, suggesting that the stronger color and texture contrast at higher temperatures facilitates the extraction of informative visual features by the CNN.

More pronounced differences are observed for the ethanol-pretreated samples (BE; panels D–F). At 60 °C (panel D), cnn1v predictions deviate from the experimental curve at intermediate times, leading to relatively high errors and a low R^2 (below about 0.40). In contrast, at 70 and 80 °C (panels E and F) the model exhibits some of its best performances, with MAE values close to 0.07, RMSE around 0.10 and R^2 exceeding 0.91. In these cases, the predicted curves closely track the experimental points over almost the entire drying period, indicating that under these conditions the visual transformations induced by ethanol pretreatment (more homogeneous darkening, pronounced surface texture) are strongly correlated with the decrease in moisture ratio.

In the combined ethanol + ultrasound pretreatment (BEU; panels J–L), the model systematically exhibits the weakest performance across all drying temperatures, with MAE values of approximately 0.15–0.18, RMSE above 0.19, and R^2 in the range of 0.62–0.66. This behavior indicates a reduced identifiability of moisture-related visual features under highly modified structural conditions.

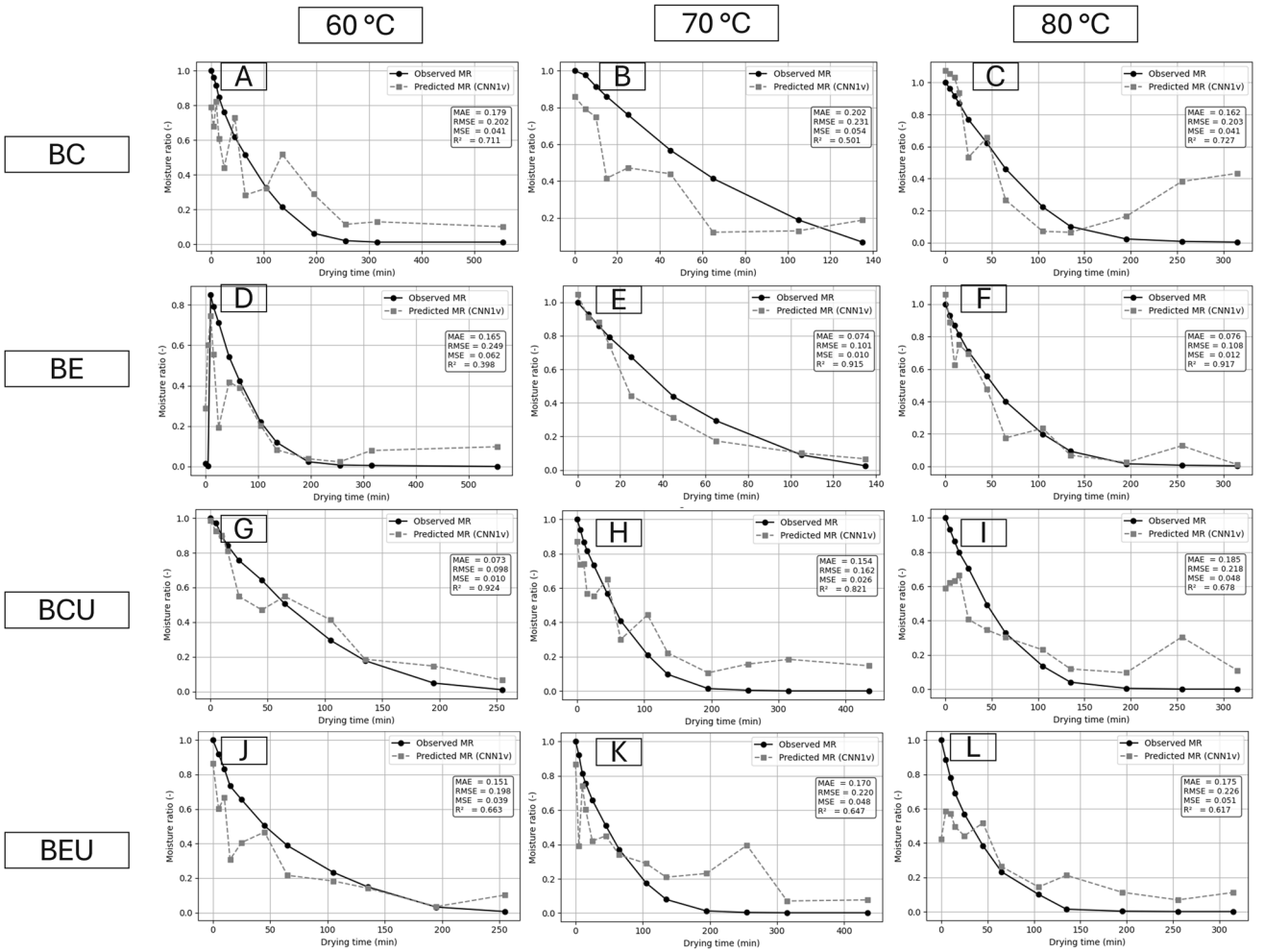


Fig. 4 Observed and CNN-predicted moisture ratio (MR) as a function of drying time for beetroot cubes under different pretreatments and air temperatures. Rows correspond to pretreatments: control (BC, panels A–C), ethanol (BE, panels D–F), ultrasound in water (BCU, panels G–I) and combined ethanol + ultrasound (BEU, panels J–L). Columns correspond to air temperatures of 60, 70 and 80 °C, respectively. In each panel, solid circles and solid lines represent the experimental MR, while open squares and dashed lines represent the MR predicted by the cnn1v model. The insets report the error metrics (MAE, RMSE, MSE and R^2) for each pretreatment–temperature combination

From a mechanistic perspective, the simultaneous application of ethanol and ultrasound induces pronounced and spatially heterogeneous microstructural changes, including localized collapse, non-uniform shrinkage, and irregular redistribution of pigments and surface moisture. These effects weaken the typically monotonic relationship between surface appearance and internal moisture content observed in the other pretreatments, thereby reducing the consistency of RGB-based moisture representations.

As a consequence, the BEU condition leads to a partial decoupling between optical surface descriptors and internal mass transfer dynamics, limiting the ability of the cnn1v model to learn a stable and generalizable mapping in this regime. This explains the increased prediction variability observed in the corresponding drying curves.

Overall, the results in Fig. 4 confirm that the cnn1v performance is strongly condition-dependent. Higher predictive accuracy is achieved for BE at 70–80 °C and BCU at 60 °C, whereas reduced performance is observed for BEU across all temperatures. These findings are consistent with recent studies on non-destructive optical monitoring of drying and highlight that model performance depends not only on learning architecture, but also on the interplay between product microstructure, pretreatment, and drying conditions.

In more detail, each of these optical studies illustrates a different way of exploiting rich spectral or thermal information to track moisture-related changes during and after drying. Jimoh et al. [13] used a visible–near-infrared HSI system (450–998 nm) to monitor glutinous rice during hot-air drying, predicting moisture content (MC), color change (ΔE) and a golden index (GI) from pixel-wise spectra coupled with wavelength-selection algorithms (CARS, IRIV, VCPA, VISSA) and non-linear regressors such as Gaussian process regression (GPR). Their best chemometric pipelines

(e.g. SG1D–IRIV–GPR and SG1D–VCPA–GPR) reached R^2 values above 0.95 for MC and above 0.90 for ΔE and GI, with very low RMSEP and mean absolute percentage deviations, and were able to reconstruct spatial maps of grain quality across the drying tray. In a complementary study, Ageh et al. [14] extended the use of the same VNIR snapshot camera to follow glutinous rice from drying through six months of storage under different temperature regimes, showing that a tuned Random Forest model based on HSI reflectance could predict milling-quality metrics (head rice yield, broken rice yield and milled rice yield) with $R^2 \approx 0.995$ and that the optimal combination for preserving value was drying at 60 °C followed by frozen storage at -10 °C.

For high-oil desiccated coconut, another study combined a novel sequential hybrid dryer with VNIR HSI (400–1002 nm) to estimate MC during processing. Using multiplicative scatter correction (MSC) and partial least squares regression (PLSR), the authors reported calibration and prediction coefficients of determination above 0.97 ($R_c^2 = 0.9784$, $R_p^2 = 0.9728$) and high residual predictive deviation (RPD), indicating excellent quantitative performance even under the complex coupled heat–mass transfer of hybrid drying [15]. Besides point predictions, hyperspectral images were used to visualize moisture gradients across the product layer, reinforcing the value of spatially resolved sensing for detecting local over- or under-drying.

At the product scale of individual slices, Bai et al. [16] employed line-scan HSI to monitor the vacuum freeze drying of *Agaricus bisporus* mushrooms, again treating MC as the target variable. After spectral pre-processing (MSC) and wavelength reduction via SCARS, they compared several regressors and found that a support vector machine (SCARS–MSC–SVM) model offered the best compromise, with $R_c^2 = 0.9281$, $R_p^2 = 0.9025$ and RPD of 2.08 for MC prediction. False-color MC maps derived from the model highlighted pronounced edge–core differences during sublimation and secondary drying, illustrating how spectral imaging can reveal internal mass-transfer phenomena that are invisible to conventional RGB imaging.

Moving beyond the visible and NIR spectrum, recent work on apple slices has introduced "thermal diffusivity phenomics" as an alternative route for non-destructive MC estimation. In this approach, samples are subjected to a controlled heating–cooling cycle while an infrared camera records time-resolved surface temperature fields; from these data, effective thermal diffusivity and related indices are extracted and linked to MC via multiple linear regression and artificial neural networks [17]. The best models achieved $R^2 > 0.90$ for MC prediction and were shown to be less sensitive to surface color or pigmentation than optical methods, while relying on lower-cost thermal cameras and simple excitation protocols. This line of work underscores that thermal transport properties can act as robust proxies for water status, particularly in products where color is not strongly correlated with moisture.

Taken together, these studies demonstrate that when rich spectral or thermal signatures are available and paired with carefully engineered chemometric pipelines, very high predictive accuracies for MC and related quality traits ($R^2 \gtrsim 0.9$) are attainable across different products, drying technologies and even extended storage. In contrast, the cnn1v model in the present work operates with a far more constrained information set, three broad RGB channels acquired with a consumer-grade camera, yet still manages to recover meaningful drying trajectories for several pretreatment–temperature combinations.

Performance of the cnn1v model for predicting moisture ratio

The convolutional neural network cnn1v was trained to regress the mean moisture ratio directly from RGB images of individual beetroot cubes. On the independent test subset, the model achieved a mean absolute error (MAE) of 0.29, a root mean squared error (RMSE) of 0.32, a mean squared error (MSE) of 0.10, and a coefficient of determination (R^2) of approximately 0.29. These global metrics indicate that, although the model captures the overall decreasing trend of moisture ratio during drying, a significant portion of the variability remains unexplained when all experimental conditions are aggregated.

Inspection of the simulated drying curves (cnn1v-predicted *rm_mean* versus drying time) confirms that the model reproduces the general sigmoidal drying behavior, including the initial rapid moisture loss followed by a progressively slower approach to equilibrium. However, deviations are observed primarily at intermediate drying stages, varying across pretreatment–temperature combinations. These deviations are attributed to combined effects of limited dataset size, within-condition variability in cube morphology (e.g. shrinkage and surface roughness), and the exclusive use of RGB images without explicit process variables such as temperature or mass loss.

This discrepancy between global and condition-specific performance reflects the inherent characteristics of drying kinetics modeling in heterogeneous systems. In convective drying processes, temperature is the dominant driving variable of moisture transport, and analyses are typically performed on a condition-specific basis. Additionally, material-dependent factors such as sample geometry, thickness, and pretreatment-induced structural changes introduce

further variability in both mass transfer dynamics and surface appearance.

Within this context, the cnn1v model learns condition-dependent mappings between RGB features and moisture ratio rather than a single global functional relationship. As a result, variability in predictive performance across conditions is expected and reflects the physical heterogeneity of the system, including differences in transport mechanisms and surface evolution patterns.

A condition-wise evaluation (Fig. 4) confirms this behavior, showing higher predictive accuracy for specific pretreatment–temperature combinations and reduced performance in more structurally heterogeneous cases. Therefore, global metrics should be interpreted together with condition-specific results, which provide a more physically meaningful representation of model performance in complex drying systems.

From an interpretability perspective, the current analysis based on early convolutional feature maps provides only qualitative insights into the cnn1v decision process. These visualizations suggest that the model captures edges and texture-related features associated with drying progression, but do not allow precise localization of the image regions driving the predictions. This limitation is more pronounced under heterogeneous conditions such as BEU (combined ethanol + ultrasound pretreatment), where complex structural changes occur during drying. More advanced attribution methods, such as Grad-CAM, could provide more detailed spatial interpretation of the learned features in future studies.

Nevertheless, this work focuses on demonstrating the feasibility of RGB-based moisture prediction using a lightweight CNN, with interpretability considered at an exploratory level.

Comparison with other imaging and machine learning approaches

When compared with state-of-the-art optical sensing and machine learning approaches, the performance of cnn1v is modest but still encouraging, considering that it relies solely on three-band RGB data acquired with a conventional camera. Hyperspectral imaging (HSI) combined with advanced machine learning has achieved much higher predictive accuracy for moisture content in various plant-based products. For sweetpotatoes, Yang et al. [12] integrated visible–near-infrared HSI (400–1000 nm) with wavelength selection and non-linear regression, obtaining R^2 values up to 0.97 and RMSE as low as 0.066 for moisture content prediction, while also estimating textural attributes such as firmness and consistency. Likewise, Tayyab et al. [8] used HSI and 3D point cloud imaging to track moisture content and quality attributes (carotenoids, anthocyanins, vitamin C, shrinkage and colour) during drying of purple carrot and golden kiwifruit, reporting prediction coefficients (R_p^2) of 0.965–0.989 for moisture content and strong agreement between optical and reference measurements.

Alternative non-contact techniques, such as near-infrared HSI and terahertz time-domain spectroscopy (THz-TDS), have also demonstrated excellent performance for real-time monitoring of moisture loss. In microwave vacuum-dried banana slices, Fu et al. [10] reported R_p^2 up to 0.98 with ratio-of-performance-to-deviation (RPD) values above 3.0 for moisture content loss prediction using partial least squares regression on NIR-HSI and THz-TDS spectra, while simultaneously evaluating the impact of non-thermal pretreatments on drying efficiency and color preservation. In another line of research, Aghili et al. [11] developed a laser light backscattering imaging (LLBI) setup for quince slices and combined color, shape and deep features extracted via pre-trained CNNs (ResNet50 and VGG19) with artificial neural networks, achieving $R_p^2 = 0.92$ and RMSEP of 7.24% for moisture content prediction.

Implications and future developments

From an application standpoint, cnn1v illustrates the potential of low-cost computer vision to complement more sophisticated sensing technologies in postharvest drying. While HSI and LLBI offer superior accuracy and rich spectral information, they require specialized hardware and higher computational resources, which can hinder adoption in small- and medium-scale processing facilities. Recent studies have suggested that carefully designed multispectral systems, using a limited number of informative wavelengths, can approximate HSI performance and lower system complexity, paving the way for practical smart dryers. The RGB-based cnn1v model can be viewed as an extreme case of such simplification, relying on three broad spectral bands and learning complex feature hierarchies directly from images.

The present results also point to several opportunities for improving cnn1v. First, expanding the image dataset and balancing the number of samples across pretreatments and temperatures should reduce overfitting and improve generalization. Second, incorporating transfer learning with deeper architectures pre-trained on large-scale image databases, as done for feature extraction in LLBI-based moisture prediction, may allow the network to exploit more discriminative representations of color and texture. Third, fusing RGB images with simple process variables (air temperature, drying time, initial mass) or with low-dimensional spectral or thermal data could enhance the sensitivity of the model to internal moisture gradients.

Overall, the combination of the visual drying panel and the cnn1v simulations provides a qualitative and quantitative link between external appearance and internal moisture dynamics of beetroot cubes dried under different pretreatments. Although the current predictive performance is lower than that of HSI- or LLBI-based approaches reported in the literature, the proposed framework demonstrates that convolutional neural networks applied to simple RGB images can already capture meaningful aspects of drying behavior, offering a promising route toward affordable, non-destructive monitoring of drying in root vegetables and other high-pigment products.

Conclusions

This work proposed a proof-of-concept approach to predict the mean moisture ratio of beetroot cubes directly from RGB images acquired during convective drying under different pretreatments and air temperatures. Analysis of drying curves by pretreatment and temperature showed that cnn1v can accurately reproduce the drying trajectory in specific conditions, with $R^2 > 0.90$ and MAE < 0.10 for ethanol-pretreated samples at 70–80 °C and ultrasound-pretreated samples at 60 °C, whereas the combined ethanol + ultrasound pretreatment was more difficult to model. Although less accurate than hyperspectral and laser-based methods reported in the literature, the proposed RGB-based CNN relies on low-cost imaging and still captures meaningful aspects of drying behavior. Overall, the results support the feasibility of using convolutional neural networks and simple RGB images for non-destructive monitoring of drying. Future work should extend the dataset, explore transfer learning and multimodal fusion with process or spectral variables to improve robustness and bring image-based moisture prediction closer to practical implementation in agro-food drying operations.

Supplementary Information The online version contains supplementary material available at https://doi.org/10.1007/s11694-026-04579-1.

Acknowledgements This work was supported by the Brazilian National Council for Scientific and Technological Development (CNPq, grant No. 306611/2022-8) and by the Pró-Reitoria de Pesquisa e Inovação (PRPI/USP) through the *Programa de Apoio aos Novos Docentes USP* (PRPI Ordinance No. 1032/2025).

Author Contributions Granella, SJ: Conceptualization; Methodology; Investigation; Data curation; Formal analysis; Software; Visualization; Writing – original draft; Writing – review & editing. Zacharias, MB: Investigation; Resources; Methodology. Moraes, TB: Funding acquisition; Resources; Supervision; Project administration; Conceptualization; Writing – review & editing.

Funding The Article Processing Charge (APC) for the publication of this research was funded by the Coordenação de Aperfeiçoamento de Pessoal de Nível Superior - Brasil (CAPES) (ROR identifier: 00x0ma614). This study received financial support from the Brazilian National Council for Scientific and Technological Development (CNPq, grant No. 306611/2022-8) and from PRPI/USP through the Programa de Apoio aos Novos Docentes USP (PRPI Ordinance No. 1032/2025).

Data Availability The datasets generated and analysed in this study are publicly available in Mendeley Data (Version 1) under the DOI 10.17632/z9hmsy6sz5.1.

Declarations

Competing Interests The authors declare that they have no competing financial or non-financial interests that could have influenced the work reported in this manuscript.

Open Access This article is licensed under a Creative Commons Attribution 4.0 International License, which permits use, sharing, adaptation, distribution and reproduction in any medium or format, as long as you give appropriate credit to the original author(s) and the source, provide a link to the Creative Commons licence, and indicate if changes were made. The images or other third party material in this article are included in the article's Creative Commons licence, unless indicated otherwise in a credit line to the material. If material is not included in the article's Creative Commons licence and your intended use is not permitted by statutory regulation or exceeds the permitted use, you will need to obtain permission directly from the copyright holder. To view a copy of this licence, visit http://creativecommons.org/licenses/by/4.0/.

References

1. X. Zeng, H. Wang, F. Zhongqi, Q. Li, H. Li, Y. Xi, W. Jiang, J. Cao, B. Liu, J. Li, Recent advances in the applications of different technologies in the processing of ready-to-eat fruit and vegetable products to improve their freshness, quality and safety: A review. Food Control. **178**, 111503 (2025). https://doi.org/10.1016/j.foodcont.2025.111503
2. F. Richter Reis, C. Marques, A.C.S. Moraes, M.L. Masson, Trends in quality assessment and drying methods used for fruits and vegetables. Food Control. **142**, 109254 (2022). https://doi.org/10.1016/j.foodcont.2022.109254
3. N.B. Silva, A. Converti, M.I.S. Maciel, Effect of ultrasound-ethanol pretreatment on drying kinetics, rehydration, quality parameters, and functional groups of BRS vitória grape using convective drying. Food and Bioprocess Technology. **18**(1), 868–880 (2025). https://doi.org/10.1007/s11947-024-03501-1
4. Z. Zang, F. Wan, G. Ma, Y. Xu, B. Wu, X. Huang, Effect of ultrasound combined with chemical pretreatment as an innovative non-thermal technology on the drying process, quality properties and texture of cherry subjected to radio frequency vacuum drying. Ultrasonics Sonochemistry. **108**, 106980 (2024). https://doi.org/10.1016/j.ultsonch.2024.106980
5. J. Cai, L. Zhu, Q. Wei, D. Huang, M. Luo, X. Tang, Drying kinetics of a single biomass particle using Fick's second law of diffusion. Processes. **11**(4) (2023). https://doi.org/10.3390/pr11040984
6. A. Szpicer, W. Bińkowska, A. Stelmasiak, I. Wojtasik-Kalinowska, A. Czajkowska, S. Mierzejewska, Z. Domiszewski, T. Rydzkowski, J. Piepiórka-Stepuk, A. Półtorak, Advances in computational fluid dynamics of mechanical processes in food engineering: Mixing, extrusion, drying, and process optimization. Applied Sciences. **15**(15) (2025). https://doi.org/10.3390/app15158752

7. T. Chuquizuta, W. Castro, M. Castro-Giraldez, P.J. Fito, Thermodynamic model and infrared thermography monitoring system for convective drying of goldenberry (*Physalis peruviana*). Journal of Food Engineering. **404**, 112773 (2026). https://doi.org/10.1016/j.jfoodeng.2025.112773
8. M. Tayyab, B. Sturm, M.A. Delele, A. Arefi, Hyperspectral and 3D point cloud imaging unraveling of physio-chemical shifts during drying of purple carrot and golden kiwifruit. Food Control. **179**, 111578 (2026). https://doi.org/10.1016/j.foodcont.2025.111578
9. C. Baltacıoğlu, M. Yetişen, H. Baltacıoğlu, A.H. Feyissa, Determination of physicochemical properties and bioactive compounds of dried apples by FTIR spectroscopy and multispectral imaging. Scientific Reports. **15**(1), 28086 (2025). https://doi.org/10.1038/s41598-025-13464-8
10. Y. Fu, Y. Ren, D.-W. Sun, Impacts of non-thermal pretreatments on banana slices during microwave vacuum dehydration using THz-TDS and NIR-HSI techniques. Journal of Food Engineering. **394**, 112518 (2025). https://doi.org/10.1016/j.jfoodeng.2025.112518
11. N.S. Aghili, S.A. Mireei, M., Sadeghi M. Jafari, R. Abbaszadeh, Novel feature extraction in laser light backscattering imaging for real-time monitoring of quince moisture content during hot-air drying. Journal of Food Engineering. **392**, 112496 (2025). https://doi.org/10.1016/j.jfoodeng.2025.112496
12. Y. Yang, N.K. Wijewardane, L. Harvey, X. Zhang, Sweetpotato moisture content and textural property estimation using hyperspectral imaging and machine learning. Journal of Food Measurement and Characterization. **19**(4), 2700–2716 (2025). https://doi.org/10.1007/s11694-025-03140-w
13. K.A. Jimoh, N. Hashim, R. Shamsudin, H. Che Man, M. Jahari, Rapid and non-destructive monitoring of the drying process of glutinous rice using visible-near infrared hyperspectral imaging. Applied Food Research. **5**(1), 100955 (2025). https://doi.org/10.1016/j.afres.2025.100955
14. O.M. Ageh, A. Dasore, N. Hashim, R. Shamsudin, H. Che Man, M. Mohd Ali, Quality monitoring of glutinous rice processing from drying to extended storage using hyperspectral imaging. Computers and Electronics in Agriculture. **225**, 109348 (2024). https://doi.org/10.1016/j.compag.2024.109348
15. Y. Sahari, M.S. Anuar, M.Z.M. Nor, N.H.A. Ghani, B.H.A. Bakar, Potential of hyperspectral imaging technology in monitoring moisture content of desiccated coconut during novel sequential hybrid drying. Agricultural Research (2024). https://doi.org/10.1007/s40003-024-00823-6
16. S. Bai, K. Xiao, Q. Liu, A.M. Mariga, W. Yang, Y. Fang, Q. Hu, H. Gao, H. Chen, F. Pei, Prediction of moisture content of Agaricus bisporus slices as affected by vacuum freeze drying using hyperspectral imaging. Food Control. **159**, 110290 (2024). https://doi.org/10.1016/j.foodcont.2024.110290
17. J.-K. Lee, M.-K. Kang, D.-H. Lee, Non-destructive prediction of apple moisture content using thermal diffusivity phenomics for quality assessment. Agriculture. **15**(8) (2025). https://doi.org/10.3390/agriculture15080869

Publisher's Note Springer Nature remains neutral with regard to jurisdictional claims in published maps and institutional affiliations.